

Modal analysis of 2-D sedimentary basin from frequency domain decomposition of ambient vibration array recordings

Valerio Poggi, Laura Ermert, Jan Burjanek, Clotaire Michel and Donat Fäh

Swiss Seismological Service, Sonneggstrasse, 5, ETH Zürich, Zürich, Switzerland. E-mail: poggi@sed.ethz.ch

Accepted 2014 October 27. Received 2014 October 27; in original form 2014 June 18

SUMMARY

Frequency domain decomposition (FDD) is a well-established spectral technique used in civil engineering to analyse and monitor the modal response of buildings and structures. The method is based on singular value decomposition of the cross-power spectral density matrix from simultaneous array recordings of ambient vibrations. This method is advantageous to retrieve not only the resonance frequencies of the investigated structure, but also the corresponding modal shapes without the need for an absolute reference. This is an important piece of information, which can be used to validate the consistency of numerical models and analytical solutions. We apply this approach using advanced signal processing to evaluate the resonance characteristics of 2-D Alpine sedimentary valleys. In this study, we present the results obtained at Martigny, in the Rhône valley (Switzerland). For the analysis, we use 2 hr of ambient vibration recordings from a linear seismic array deployed perpendicularly to the valley axis. Only the horizontal-axial direction (*SH*) of the ground motion is considered. Using the FDD method, six separate resonant frequencies are retrieved together with their corresponding modal shapes. We compare the mode shapes with results from classical standard spectral ratios and numerical simulations of ambient vibration recordings.

Key words: Site effects; Computational seismology; Wave propagation.

1 INTRODUCTION

The shape of an earthquake signal can heavily be altered during its propagation from the source to the observation point. One of the most severe modifications of the earthquake signal comes from the reverberation of the seismic wavefield in the uppermost few to 100 m of the Earth structure, where large variability of the geological and geophysical conditions is present (e.g. Borchardt 1970; Joyner *et al.* 1981; Anderson *et al.* 1996). This effect, related to the resonance of the system, is most pronounced in sedimentary basins with complex 2-D/3-D geometry and irregular topography, where strong velocity contrast exists (e.g. Bard & Gariel 1986; Geli *et al.* 1988). The interaction of the earthquake wavefield with the structure may lead to additional phenomena, such as focusing or defocusing effects of the wavefield and the development of edge-generated surface waves (e.g. Vidale & Helmlinger 1988; Field 1996; Hisada & Yamamoto 1996; Chavez-Garcia *et al.* 2000; Bindi *et al.* 2009). These phenomena are responsible for the generally larger ground-motion in sedimentary basins.

The development of 2-D resonance is to be expected in narrow, deep alpine valleys, where the seismic velocities contrast between sediment fill and underlying bedrock is high (Bard & Bouchon 1985; Steimen *et al.* 2003). The effect on ground motion can be severe, with amplification factors of 10 and more, often well localized in

delimited areas of the basin, further associated with duration of several tens of seconds, as reported by Trifunac & Brady (1975) for typical soft sediment sites. Moreover, the frequency bands in which amplification occur often match the resonant frequencies of buildings and structures, typically between 0.5 and 10 Hz (Anderson *et al.* 1986).

Despite its relevance, 2-D/3-D resonance of sedimentary basins is a hardly predictable phenomenon. Often, numerical methods are employed to model the complex 2-D/3-D-shaking scenario (e.g. Fäh & Suhadolc 1994; Frischknecht & Wagner 2004; Smerzini *et al.* 2011). In this case, however, an accurate knowledge of the subsoil structure is needed, which is frequently not available due to the rather high costs of the geophysical investigations. Direct approaches, which are based on the analysis of real earthquake events, are generally preferable (e.g. Kagami *et al.* 1982; King & Tucker 1984). In low seismicity regions, however, the lack of recordings makes such approach not always feasible.

Nowadays, direct techniques based on the analysis of the ambient vibration wavefield (often named ‘seismic noise’) have demonstrated to be convenient and reliable alternative to the conventional seismic methods to infer important information on the underground structure. Most common ambient-vibration techniques are the single station horizontal-oververtical Fourier spectral ratio (or H/V, see Bonnefoy-Claudet *et al.* 2006 for an exhaustive reference list)

and the family of array techniques (f - k and SPAC, e.g. Asten & Henstridge 1984; Asten 2006; Poggi & Fäh 2010). The former approach allows a fast and relatively precise estimation of the SH -wave fundamental frequency of resonance (f_0) of the site (Lachet & Bard 1994), while the latter group is useful to retrieve the velocity structure of the site (mainly S -wave velocity as a function of depth, and to a lesser extent P -wave velocity) by inversion of observed surface wave dispersion curves.

Ambient vibration can be used to directly characterize the resonance behaviour of the sedimentary basins, for example by mapping the variations in the fundamental frequency of resonance over extended areas in shallow basins (e.g. Ibs-von Seht & Wohlenberg 1999; Guéguen *et al.* 2007; Le Roux *et al.* 2012; Poggi *et al.* 2012), or by identifying 2-D resonances using techniques such as site-to-reference spectral ratios (also called standard spectral ratios, SSR, e.g. Yamanaka *et al.* 1993; Lermo & Chavez-Garcia 1994; Roten *et al.* 2006). This last approach, however, can only provide rough nodal information of the resonant mode shapes, which is essential to discriminate and sort the system eigenfunctions. Moreover, the frequency resolution of the amplification peaks is usually insufficient to determine more than the lowest two eigenfrequencies (Roten *et al.* 2006). This is often due to the difficulty in selecting the appropriate location for the reference station; the ambient vibration wavefield outside the basin might not be sufficiently correlated with the inner recordings, while inside it might be difficult to fully remove the input motion from the system response.

In order to improve the measurement of mode shapes and nodes, the frequency domain decomposition (FDD) method (Brincker *et al.* 2001) is applied to synchronous array recordings of ambient vibration. The FDD method is a popular seismic technique used in mechanical and civil engineering for system response analysis. It basically relies on singular value decomposition of the signal's cross-power spectral density matrix to retrieve the eigenfunctions of the system. With this method, once a resonance frequency is identified by a maximum in the signal cross-power spectrum, the corresponding eigenvector is extracted and interpreted as representative of the modal shape of the system at that frequency.

FDD method has been first applied to borehole seismic array recordings by Guéguen *et al.* (2011) for the evaluation of the 1-D seismic response of the soil column. The same approach has later been applied to complex geological structures by Ermert *et al.* (2014) to observationally characterize the resonance of 2-D alpine sedimentary basins. In this paper, we validate the method on a theoretical base from a seismological perspective and by comparing results from real recordings to numerical simulations of ambient vibrations. We first test the method on a dataset previously acquired by Roten & Fäh (2007) in Martigny (Rhône valley, Switzerland, Fig. 1). Nearly 2 hr of three-component recording are available from the experiment, which consists in a linear array of three-component seismometers deployed along the transversal section of the basin. We analyse the axial (or SH) ground motion direction of the valley. Both SSR and FDD techniques are applied to the recordings in the frequency range 0.1–1 Hz and under the assumption of dominant 2-D resonance behaviour in the wavefield. With FDD, up to six separate resonant frequencies are identified with a clear corresponding modal shape, which is not possible with SSR. The same processing scheme (SSR and FDD) is subsequently applied to a set of stochastically generated synthetic recordings of ambient vibrations from 2-D numerical simulation of the Rhône valley. Theoretical results are then compared to observations, in order to investigate the robustness of the method and of the working assumptions.

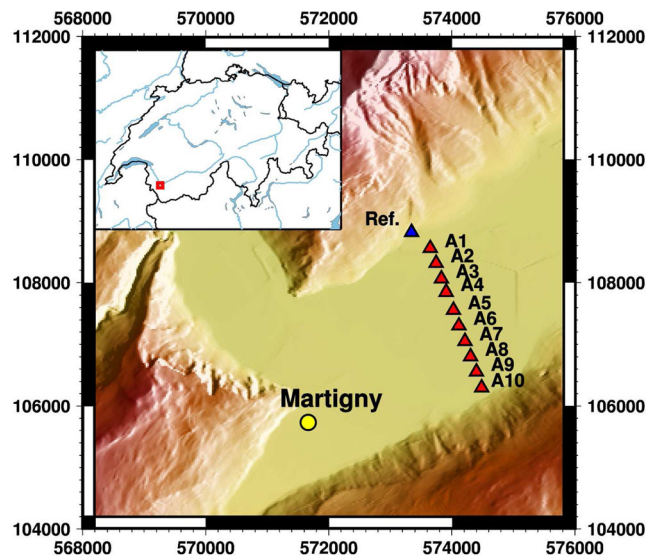


Figure 1. Deployment of the linear array of 10 three-component seismological stations in the Rhône valley (Switzerland) close to Martigny (Roten & Fäh 2007). The reference station (in blue) used for the SSR method is also shown, but not used for the analysis with FDD. Units are metres on the Swiss coordinate system (CH-1903).

2 WORKING ASSUMPTIONS AND NAMING CONVENTION

In a theoretical 2-D case, the perpendicular or in-plane (P - SV) and axial or out-of-plane (SH) components of ground motion are separated (orthogonal) and do not interact with each other. Such a representation is an advantageous simplification, as it allows a more compact treatment of the wave propagation phenomena, separately for the two directions. In this study, in particular, we focus on the axial (SH) direction of motion, whose results are easier to interpret. This is done in order to validate the reliability of the FDD method.

Elongated alpine valleys can be considered a good approximation of 2-D structures. In this case, the SH component is namely oriented along main axis of the valley, while P - SV lies on its cross section. Development of SH resonance modes in a 2-D environment can be described using the naming convention proposed by Bard & Bouchon (1985). According to this formalism, modes are progressively sorted using an incremental two indexes approach; first index always describes the number of nodes at the surface along in the horizontal (x) direction, while second index enumerates the nodes on the vertical (z) axis (e.g. Fig. 2).

3 FDD

The FDD method is a spectral technique introduced by Brincker *et al.* (2001) to characterize and monitor the system response of mechanical systems and civil structures, such as buildings (e.g. Michel *et al.* 2010) and bridges (e.g. Goulet *et al.* 2013), when excited by an unknown stochastic input. The method relies on the acquisition of synchronous signals from multiple (array) recordings. As main advantage compared to other response analysis techniques such as the transfer function method, this technique does require neither a reference outside the system nor the prior knowledge on the loading forces, as the system response contributions are separated from the recorded motion by factorization of the signal's cross-power spectral matrix. As a major assumption, the presence of a stochastic (diffuse) wavefield can be associated to a random

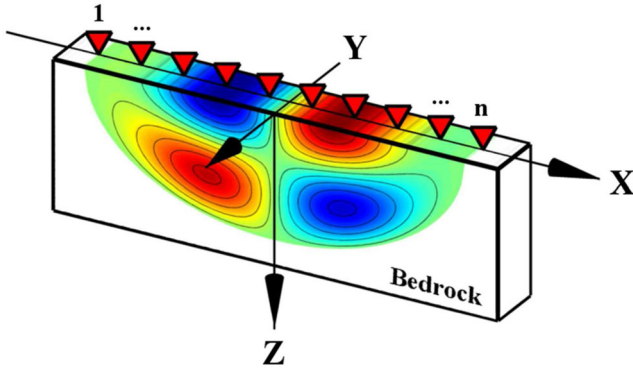


Figure 2. Schematic representation of 2-D resonance in a simplified sedimentary valley section. In this example the displacement of the SH_{11} resonant mode is shown with colour (rigid bedrock is assumed). On the free surface, the ground motion is sampled by a seismic array of n stations (red triangles).

distribution of sources in space and time. Therefore, the method theoretically suits well with the recording of ambient vibrations.

In the following, we present the basic principles of the method using formalism suitable to describe wave propagation in a 2-D sedimentary basin. For a more general description of the method we refer to Brincker *et al.* (2001).

As first, we consider a simplified description of a 2-D valley as in Fig. 2. We assume the presence of a certain number of noise sources randomly distributed, whose wavefield excites the resonance modes of the structure at discrete resonance frequencies. Because of the simplification to the 2-D case, the axial contribution of the wavefield (SH) does not interact with the perpendicular motion ($P-SV$), so that we can restrict our analysis either to the SH or the $P-SV$ case independently. In this case, we focus on the SH motion, which is easier to treat mathematically.

In our model, n measuring locations (the seismic receivers) are deployed in a linear array on the free surface of the valley. Equal spacing between receivers is not a necessary condition, but it is a convenient simplification. If we restrict our analysis in the narrow frequency band around a resonance frequency of the basin ($\omega = \omega_0$), the ground motion related to the associated mode shape can be modelled at each receiver location as a harmonic spatially stationary signal modulated with a modal shape function, which only depends on the resonance frequency and the spatial coordinates of the receiver:

$$U_{SH}(x, t) = P(\omega_0)M(x, \omega_0) \cos(\omega_0 t + \varphi) + \eta(x, t), \quad (1)$$

where $P(\omega_0)$ is the energy of the signal, $M(x, \omega_0)$ is the mode shape along the valley at the resonance frequency ω_0 , φ is the initial phase and $\eta(x, t)$ is some additive realization of uncorrelated noise.

In the frequency domain and at the frequency corresponding to that specific resonant frequency ω_0 , eq. (1) can be identically represented as:

$$U_{SH}(x, \omega_0) = P(\omega_0)M(x, \omega_0)e^{-j\varphi} + \eta(x, \omega_0). \quad (2)$$

Considering all the n discrete receiver locations of the array, the ground motion can be similarly expressed in a more compacted vector notation as:

$$\begin{aligned} \vec{U}_{SH}(\omega_0) &= [U_{SH}(x_1, \omega_0), U_{SH}(x_2, \omega_0), \dots, U_{SH}(x_n, \omega_0)]^T \\ &= P(\omega_0)\vec{M}(\omega_0)e^{-j\varphi} + \vec{\eta}(\omega_0), \end{aligned} \quad (3)$$

where T stands for transpose.

Note that, as the modal shape vector should not carry any signal energy information, the following has to be satisfied:

$$\|\vec{M}(\omega_0)\| = 1. \quad (4)$$

The cross-power spectral density matrix $\hat{C}(\omega_0)$ can then be obtained by computing the expected (E) value of all the cross-products between pairs of receivers along the array (as a further notation simplification, the dependency on frequency is implicitly assumed):

$$\begin{aligned} \hat{C}(\omega_0) &= E \left[\vec{U}^{SH} (\vec{U}^{SH})^h \right] \\ &= E \left[P^2 \vec{M} \vec{M}^h + P \vec{M} \vec{\eta}^h e^{-j\varphi} + P \vec{\eta} \vec{M}^h e^{j\varphi} + \vec{\eta} \vec{\eta}^h \right], \end{aligned} \quad (5)$$

where h stands for Hermitian transpose (complex conjugate). Computing the expectation under the justified assumption that noise and signal are uncorrelated, the mixed terms from the cross-product with the noise vector vanish (Poggi & Fäh 2010). Similarly, assuming that the uncorrelated noise is a zero mean Gaussian process with variance σ^2 , the last term of eq. (5) reduces to the product of the noise variance times an identity matrix \hat{I} of size $n \times n$ (n being the number of receivers):

$$\vec{\eta} \vec{\eta}^h \cong \sigma^2(\omega_0) \hat{I}. \quad (6)$$

Therefore, the cross-spectral density matrix simplifies to:

$$\hat{C} \cong P^2 \vec{M} \vec{M}^h + \sigma^2 \hat{I}. \quad (7)$$

The cross-power spectral density matrix is positive semi-definite and Hermitian; its singular value decomposition can be expressed in the form:

$$\hat{C} = \hat{V} \hat{S} \hat{V}^h, \quad (8)$$

where \hat{S} is the diagonal matrix of the real eigenvalues and \hat{V} is the matrix of eigenvectors. By substituting eq. (8) in eq. (7) and moving the noise contribution to the left-hand side we then obtain:

$$\hat{V} \hat{S} \hat{V}^h - \sigma^2 \hat{I} \cong P^2 \vec{M} \vec{M}^h. \quad (9)$$

Because of the orthogonal property of the eigenvector matrix ($\hat{V} \hat{V}^h = \hat{I}$), eq. (9) can be then rewritten as:

$$\hat{V} \hat{S} \hat{V}^h - \hat{V} (\sigma^2 \hat{I}) \hat{V}^h = \hat{V} (\hat{S} - \sigma^2 \hat{I}) \hat{V}^h \cong P^2 \vec{M} \vec{M}^h. \quad (10)$$

From eq. (10) is then clear that the eigen-decomposition of \hat{C} directly provides an estimate of the modal function and the signal power at the analysed frequency. In the ideal case where a single signal is present at frequency ω_0 , the eigenvalue matrix can be reduced to a scalar corresponding to unique non-zero eigenvalue S_1 , while the eigenvector matrix has the only significant eigenvector corresponding to S_1 .

$$\begin{cases} \vec{V}_1 = \vec{M} \\ S_1 \cong P^2 + \sigma^2 \end{cases} \quad (11)$$

If the noise variance is much smaller than the signal amplitude ($P^2 \gg \sigma^2$), the noise contribution to the eigenvalue (or power) spectrum can simply be neglected. If not, an additive amplitude factor has to be accounted for. Moreover, suppression of uncorrelated noise contribution by expectation is in reality never perfect (because of the finite nature of the time series), leading therefore to progressively biased results, especially for low energy overtones. The frequencies at which resonance occurs are generally unknown *a priori*; nonetheless these can be identified by locating correlation maxima on the eigenvalue spectrum computed for a reasonable frequency range. After that, resonant mode functions can be identified

and extracted by the analysis of the corresponding complex eigenvectors. In practice, the imaginary part is dropped, while the real part fully characterizes the modal shape.

It has to be mentioned that, in reality, several modes and more signals can impinge and overlap at each frequency. Under the assumption that close modes are orthogonal in space and the attenuation small, exact modal shapes can still be retrieved (Brincker *et al.* 2001). As well, the noise level might be significant and a certain degree of correlation can be present between noise and resonant modes. Nevertheless, also in such a case singular value decomposition of the cross-power spectral density matrix can be helpful in separating out the different modal contributions. Here, the different modal functions are ordered through their eigenvalues, depending on the energy level and the coherence of the analysed modal signal.

4 MODAL ANALYSIS OF THE RHÔNE VALLEY USING AMBIENT VIBRATIONS

The FDD method has been tested on approximately 2-hr ambient vibration recordings from a linear array performed by Roten & Fäh (2007) in the Rhône valley close to Martigny (Figs 1 and 2). In the following section, we present the most relevant information about the experiment setup and describe the main processing steps and results obtained from modal analysis using FDD. A comparison with the application of SSR method is also presented, to better highlight the improvements achieved.

4.1 Geological settings

The Rhône valley is a deeply incised alpine valley of glacial origin. From the tectonic point of view, the study area lies on the Penninic front, which separates the sedimentary units of the Helvetic domain (to the north) from the high-grade metamorphic rocks of the Penninic nappes (towards South). The crystalline basement is in many areas largely exposed (Mont Blanche massif). More specifically, in the Martigny region the geophysical bedrock is mostly constituted of gneiss and schists.

A high-resolution seismic reflection study conducted during a national research project (NRP20, Pfiffner *et al.* 1997) revealed the geometrical complexity of the valley, which exhibits an asymmetric geometry and a mixture of U- and V-shaped transversal sections. Some parts of the valley are strongly overdeepened, so that the glacial and postglacial quaternary deposits forming the valley fill reach thicknesses of up to about 900 m. Geological interpretations (Fig. 3) of the seismic survey NRP20 and the analysis of local borehole logs indicate that the unconsolidated sediments fill (mostly

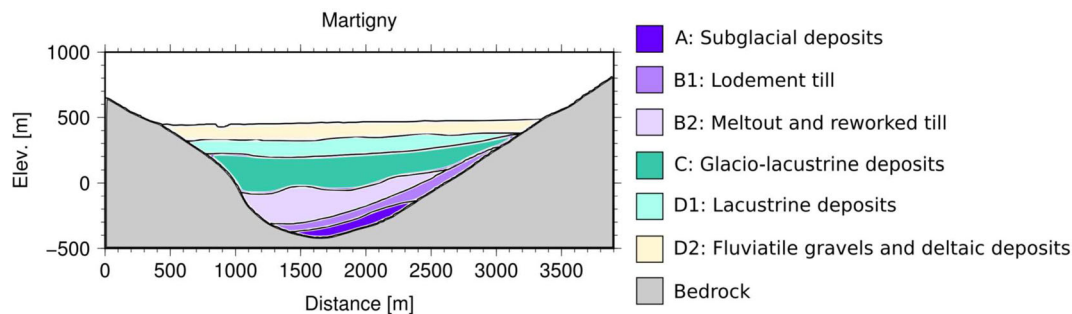


Figure 3. Geological cross-section of the Rhône valley close to Martigny (modified from Pfiffner *et al.* 1997). The bedrock is typically asymmetric, but with a nearly flat horizontal layer infill (with the exception of unit A and B1 at the southern edge).

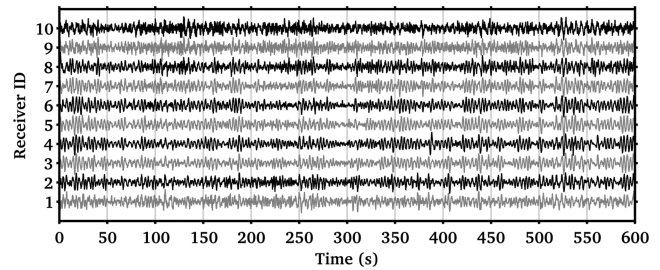


Figure 4. Example of 10 min of ambient vibration recordings (horizontal-axial direction of the valley axis) from the Martigny linear array in Fig. 1. No evidences of relevant transients of anthropogenic origin are visible on the traces, as reported at other sites in the Valais region.

till and fluvio-lacustrine deposits) can be related to the last glacial maximum (Pleistocene).

4.2 The ambient vibration linear array

The data set consists in 1 hr 50 min of synchronous three-component recordings of ambient vibration from a linear array deployed perpendicularly to the valley axis. For the experiment, 10 seismological stations were used (Quanterra Q330, 24bit), equipped with triaxial velocity sensors (Lennartz 3C, 5s natural frequency). The array was designed with an extension of about 2500 m and regular spacing of approximately 200–250 m to cover the whole valley section. One additional station was deployed outside the valley border on outcropping rock, to be used as reference for standard Fourier spectral ratios. The horizontal components of the sensors were originally aligned to the N–S and E–W directions. Recordings have been later rotated to produce a set of equivalent components along and perpendicular to the valley axis (Fig. 4). The measurement setup assumes 2-D behaviour. Therefore, the proper segregation and analysis of the *SH* and *P–SV* components of the ground motion is achieved through this decomposition. In the more general 3-D case this is not necessary. GPS signals were used for time synchronization.

4.3 Ambient vibration processing using FDD and SSR

The first step of FDD processing is the estimation of the signal covariance matrix. To do this, ambient vibration recordings from the linear array were first divided in short windows of exactly 50 s, with 50 percent overlapping. Shorter and longer time windows have also been tested during the experiment, but 50 s provided the best trade-off between spectral resolution and minimization of the smearing effect from the presence of uncorrelated noise. Each window was subsequently tapered with a Tukey (cosine) function

($\alpha = 0.2$) and then the Fourier spectrum calculated in the range 0.1–1 Hz. Above and below these frequency bounds no useful results could be obtained, as we verified. A consistent windowing scheme was subsequently used for the SSR processing.

For each discrete frequency in the range, then, a number of cross-power spectral density matrices have been estimated by stacking of spectral cross-correlations over blocks of 50 consecutive windows. Stacking had the goal of minimizing the effect of the uncorrelated noise by stabilizing the phase-delay expectation between receiver pairs and enhancing the coherent part of the signal. Finally, singular value decomposition was performed for each separate block, and the eigenfunctions averaged over all consecutive blocks to improve the quality of the estimation.

It should be noticed that the phase of the eigenvectors in the complex plane is initially arbitrary. Therefore, in order to perform a proper averaging of the modal shapes without reciprocal cancellation of the eigenvectors of opposite sign, a phase correction should first be applied (Burjnek *et al.* 2010). In this study, the amount of phase rotation θ_0 is found by maximizing the length of the real part of the first eigenvector \vec{V}_1 (Vidale 1986):

$$\theta_0 = \operatorname{argmax}_{\theta \in [0, \pi]} \left\{ \sqrt{\sum_{k=1}^n [\Re(V_{1,k} \cos \theta + i V_{1,k} \sin \theta)]^2} \right\}. \quad (12)$$

The eigenvectors are finally rotated in the complex plane by the optimum angle θ_0 before averaging. Such approach showed to be advantageous as it allows a more robust estimation of the modal shapes, and eventually a better definition of the corresponding uncertainty.

4.4 Results of the modal analysis

As highlighted by Roten *et al.* (2006), processing ambient vibrations using SSR on a linear array provides only limited resolution on the 2-D resonance characteristic of the basin. In the case of Martigny, using SSR led to a clear identification of the first four *SH* resonance frequencies, up to about 0.52 Hz (Fig. 5). The reconstruction of the corresponding modal shapes is however very incomplete and at some frequencies even doubtful. Above 0.6 Hz no further information can realistically be extracted. This can partially be due to the difficulty in selecting a proper reference for SSR of ambient vibrations; when outside the basin—possibly on outcropping bedrock, as in the present case—the reference often shows low cor-

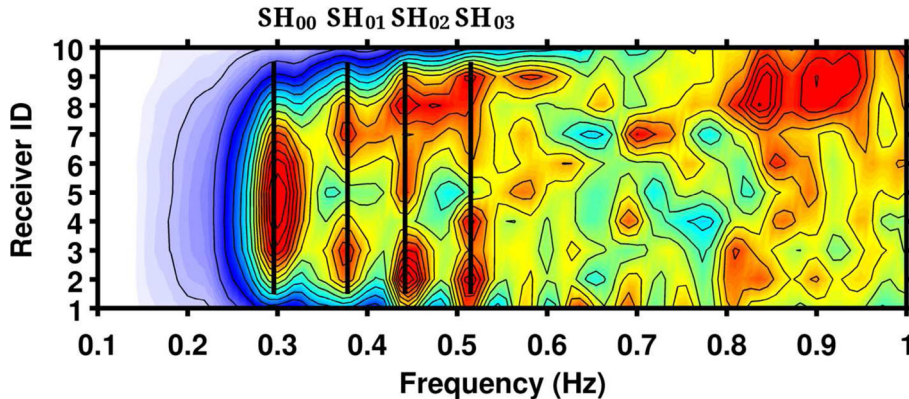


Figure 5. Interpolation of standard spectral ratio results computed for each station of the array profile in Fig. 1. The first four *SH* resonant modes are clearly identifiable in the range 0.29–0.52 Hz, while interpretation is more difficult above these frequencies. This is likely due to the presence in the ambient vibration wavefield of wave contributions (e.g. surface waves) not separable using the SSR approach.

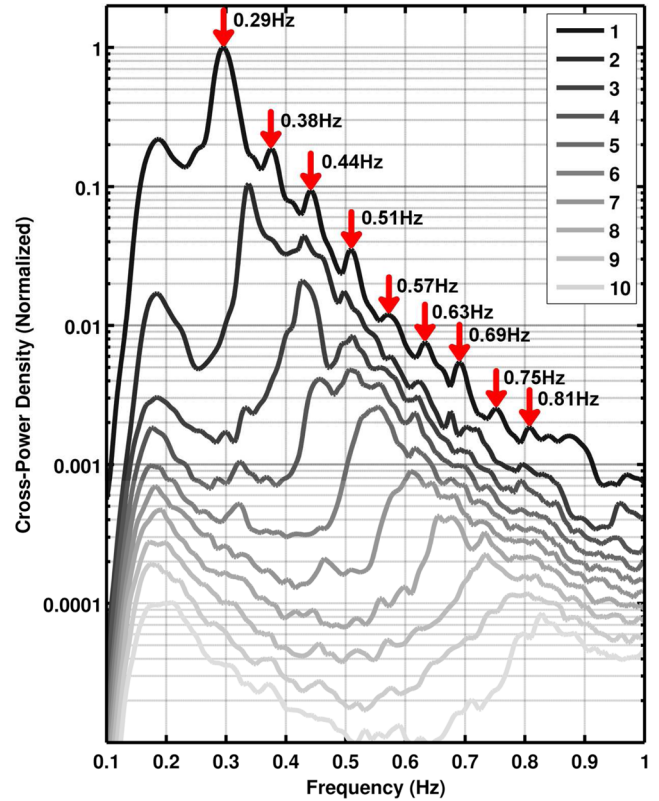


Figure 6. Cross-power density (or eigenvalue) spectrum from FDD analysis of the Martigny linear array. All the 10 eigenvalue curves are presented for comparison, while the red arrows indicate nine identified resonant modes. Note that the apparent maximum at about 0.2 Hz is only due to the corner of the instrument response and does not represent a real feature of the valley.

relation with the recordings on sediments. Conversely, a reference inside the basin might not properly remove the effect of the input motion.

Application of the FDD method provides better results. From the analysis of the eigenvalue spectrum in the range 0.1–1 Hz, at least nine separate modes are clearly evident as consecutive maxima (Fig. 6). Probably, two more modes could be identified between 0.8 and 1 Hz, but are too uncertain to be considered for further analysis. Subsequently, by evaluation of the corresponding eigenvectors at the identified resonance frequencies (Fig. 7), the related modal

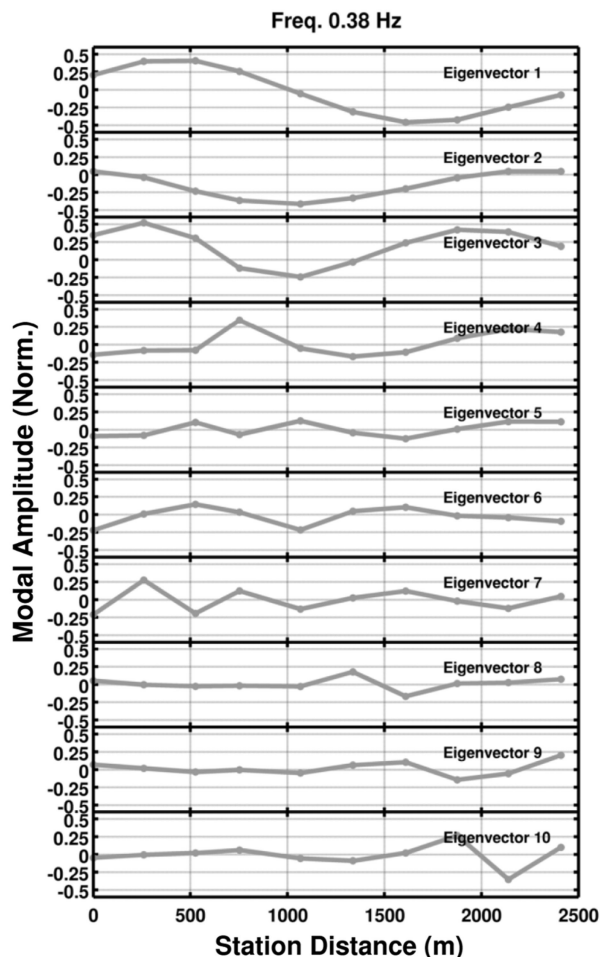


Figure 7. Example of the sequence of 10 eigenvectors (real part) for the mode identified at 0.38 Hz (2nd overtone). The first eigenvector (on top) provides the actual modal shape, but analysing the remaining eigenvectors is nevertheless useful in doubtful cases, as it provides information about low energy modes and/or about the influence of nearby frequencies.

shapes are extracted. It should be noted that, to correctly address the different modes, it is generally advantageous to analyse not only the first eigenvalue–eigenvector pair, but also the subsequent ones. This might be useful in the case of modes very close in frequency, but with rather different energy. Here, the stronger mode can hide the presence of the weaker one, and only an accurate evaluation of all the eigenvalue–eigenvector pairs might disclose it.

In the study case, modal interpretation is clear up to the 6th overtone (Fig. 8). Above that, the modal addressing starts to be problematic because of the limited spatial sampling of the resonant wavefield. Probably, having denser station coverage could have provided enough resolution to discriminate additional higher modes. As evident from Fig. 8, the six modes have progressively increasing number of nodes on the horizontal direction and are expected to be the SH_{0n} , with $n = 0–5$. Conversely, modes with nodes on the vertical direction are not resolved from this analysis. The modal shapes of the identified modes show the location along the array profile where the maximum (antinodes) and the minimum (nodes) resonance effect should be expected at a particular resonance frequency. Such a complete map of the mode shape can hardly be obtained by standard techniques such as the spectral ratio, which only presents the absolute amplitude information of the signal.

5 VALIDATION WITH SYNTHETIC RESULTS

In order to validate the reliability of the results from FDD processing, we produced a set of synthetic ambient vibration recordings aiming to emulate the linear array of Martigny. For the simulation we used a 2-D finite-differences modelling code for SH -wave propagation (SOFI2D- SH , Bohlen 2002), following a stochastic approach for the generation and superposition of randomly distributed noise sources. The numerical model of the Rhône Valley (Fig. 9) was set up collecting information from previous ambient vibration studies (Steimen *et al.* 2003; Roten *et al.* 2006; Roten & Fäh, 2007) and geophysical measurements available for the area (Pfiffner *et al.* 1997). Both sedimentary infill and bedrock were modelled as viscoelastic materials (no rigid basement assumed). Seismic velocities, densities and quality factors of the final model are summarized in Table 1. The simulated recordings have then been processed with SSR and FDD processing, and results later compared with observations from direct measurements.

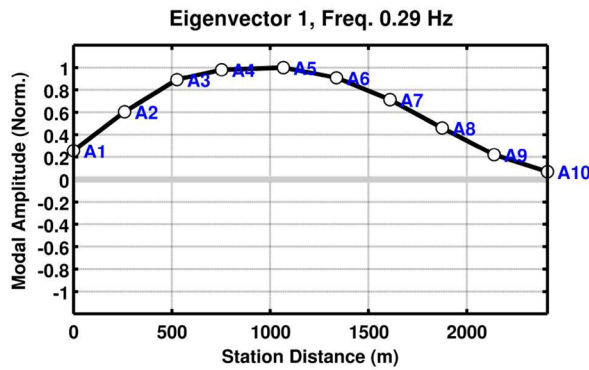
5.1 Generation of the synthetic ambient vibration recordings

To simulate synthetic ambient vibration recordings in a 2-D sedimentary environment we used a stochastic approach based on full-wave propagation modelling. At first, we produced 36 separate synthetic Green’s functions of 60 s each using a 2-D staggered-grid (on stress–velocity nodes) viscoelastic finite-difference modelling code (SOFI2D- SH , Bohlen 2002) developed at the Karlsruhe Institute of Technology (KIT). Only the axial (SH) component of motion was simulated.

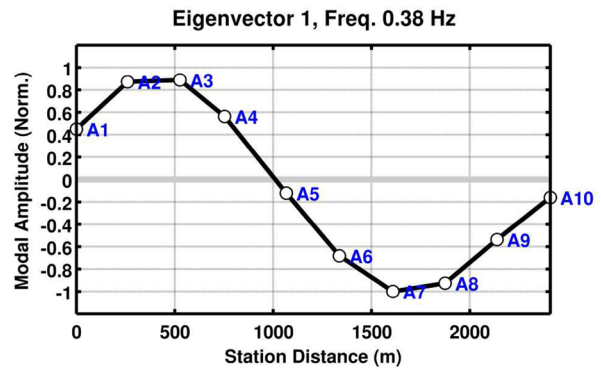
Each simulation was performed assuming a point source, distributed along an array of 36 elements with 100 m between and at fixed depth of 1200 m. Even though such source distribution can be questionable for the simulation of ambient vibration recordings—where surfaces waves are generally the target (e.g. Cornou 2004)—the approximation is suitable for our purposes, since we only focus on stochastic excitation of 2-D resonant modes of the structure. Therefore, such a linear array of sources would properly illuminate the basin from a broad set of incidence angles, as expected in the theoretical case of a pure diffuse field. The source function consisted of a Dirac pulse filtered with a 4th order anticausal low-pass filter with 2 Hz corner frequency. The simulation was limited to a frequency range between 0.1 and 1 Hz, imposed considering the expected resonance characteristics of the target site. Time step (0.001 s) and grid size (800×300 gridpoints with 5 m distance between) of the numerical model were defined according to maximum frequency and minimum wavelength of the simulation. Absorbing boundaries were dimensioned (200 m width with 5 per cent damping) in order to avoid any influence of the model borders on the resonance behaviour of system. The receiver array consisted of 36 elements located at the surface of the model with 100 m between them.

By then stacking 1000 random realizations of those 36 synthetic Green’s functions we generated 600 s of ambient vibration recordings (Fig. 10). Before stacking, each realization was modulated adding certain random time delay (0–600 s) and random amplitude (from 0.5 to 1, normalized units), to properly account for the stochastic composition of the ambient vibration wavefield. No additional uncorrelated noise was superposed on the final recordings.

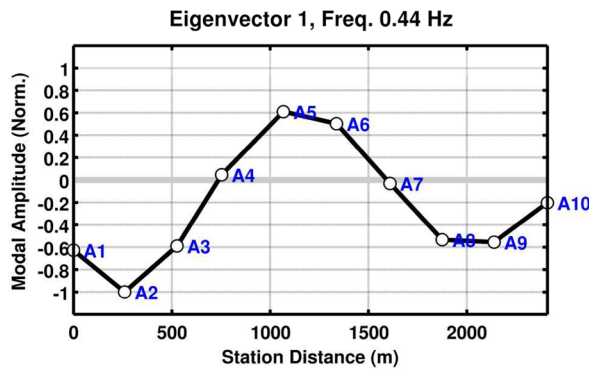
1) SH₀₀



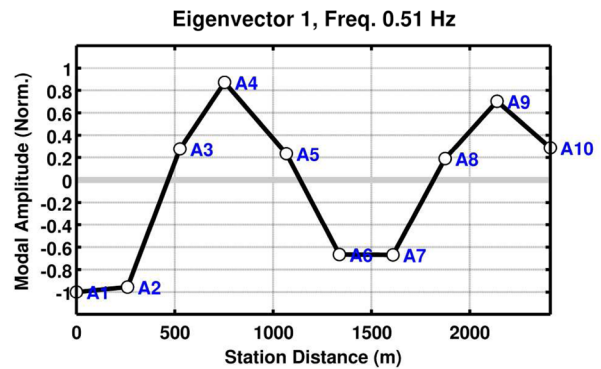
2) SH₀₁



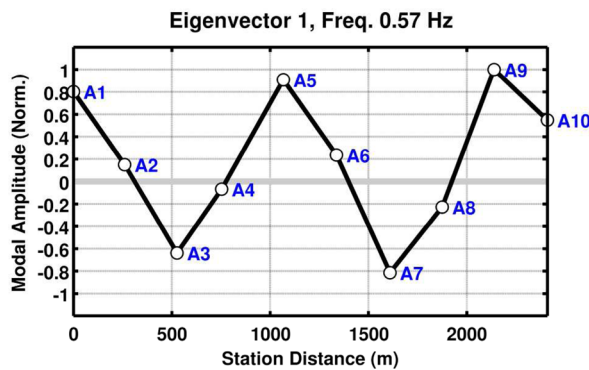
3) SH₀₂



4) SH₀₃



5) SH₀₄



6) SH₀₅

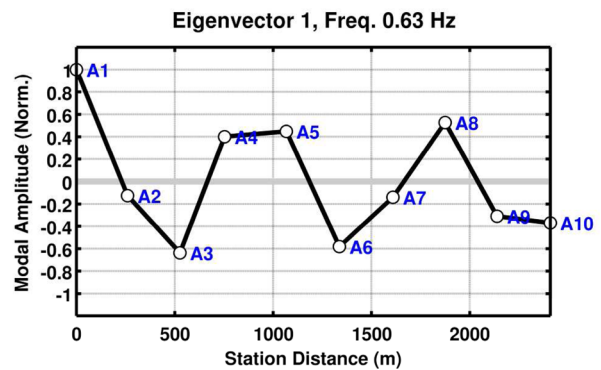


Figure 8. Modal shapes (real part of the first eigenvector) of the first six modes identified on the power-spectrum of Fig. 6. White dots indicate the receiver location along the array. Nodes and antinodes can be easily identified for each mode. Above the fifth overtone it is not possible anymore to correctly reconstruct the modal shape, due to the insufficient spatial sampling.

5.2 SSR and FDD processing of synthetic recordings

In order to validate the method, the simulated ambient vibration recordings were processed, as for the real case, using both SSRs (Fig. 11) and FDD (Fig. 12). For better comparison, the processing parametrization scheme was defined as close as possible to that used with observed recordings. Some differences were nevertheless present, principally due to different length of the recordings. This has a direct impact on the number of windows stacked for the estimation of the signal correlation matrix. Consequently, in order to test the sensitivity of window number/length on eigenfunction resolution, some alternative parametrizations have also been examined (e.g. A, B and C of Fig. 12, Table 2) and results compared.

Synthetic recordings were computed in the frequency range from 0.1 to 1 Hz. In the low-frequency part of the simulation (<0.6 Hz) we found good agreement with observed results, while at high frequencies (>0.6 Hz) progressive deviations have been spotted. These deviations are nevertheless addressable mostly to the oversimplification of the numerical model, especially related to the uncertainty on velocity distribution and the unknown quality factors. As highlighted by Ermert *et al.* (2014) using numerical modal analysis, differences in model characteristics can significantly affect the development of higher modes. In the case of Martigny, modes above the fourth overtone might be too strongly dependent on the uncertain structural characteristics of the model (especially in the first

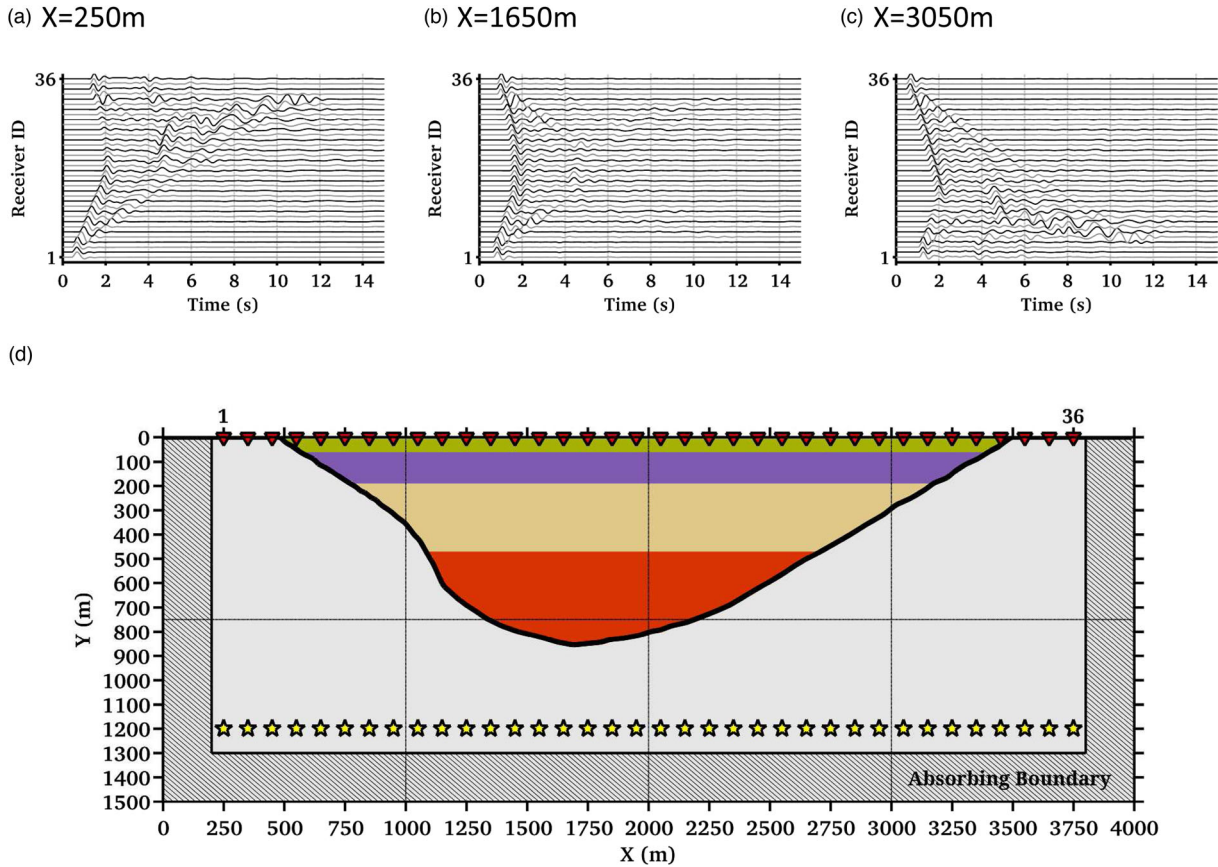


Figure 9. (a–c) Example of simulated Green's functions for three source locations at same depth (1200 m) but different horizontal position along the profile. (d) 2-D numerical model of the Rhône valley. The sediment infill consists of four flat-horizontal layers with velocity increasing with depth (see Table 1). The 36 source locations are presented with yellow stars, while receivers are indicated with red triangles.

Table 1. Parameters of the numerical model of Martigny. Values are modified from Roten & Fäh (2007).

	Thickness (m)	S velocity (m s^{-1})	Density (kg m^{-3})	Quality factor
1st Layer	50	277	1900	25
2nd Layer	130	443	2000	25
3rd Layer	280	620	2000	25
4th Layer	540	828	2000	25
Bedrock	–	2890	2500	100

tens of metres) to produce a meaningful comparison. Consequently, since in this study we only target the validation of the FDD approach on 2-D geological structures, results for frequencies above 0.6 Hz are not presented and further discussed for the sake of conciseness.

SSR and FDD provided the same frequency values for the first four modes of resonance (Table 3). With respect to observations, simulated recordings provided a slightly lower value for the fundamental mode and the first overtone. This is likely related to the incomplete knowledge of the model, particularly the simplified flat layering and the uncertainty on the correct bedrock depth and shape. As expected, SSR provided better results with synthetic than with real recordings. This is possibly due to the high coherency of the simulated wavefield and the use of a proper reference, which sits on ideal bedrock and carries unbiased information of the input motion. However, this is hardly expected in real case. Eigenvalue spectrum (Fig. 12) and mode shapes (Fig. 13) from FDD are consistent with observations. In particular, a very satisfactory approximation is ob-

tained for the mode shapes, including both nodal and antinodal point locations. As in the case of individual frequency values, small deviations on mode shapes can be addressed to the simplification of the numerical model and to the epistemic uncertainty on the model parameters. Such differences are nevertheless negligible, given that any model can hardly give resolution as good as direct experimental analysis.

Result of FDD processing might be subsequently used to refine the structural characteristics of the model. Modal shapes, for instance, might be used as additional constrain for the inversion of the bedrock shape, or as direct proxy to highlight asymmetries and heterogeneities of the sedimentary structure. Complementary, higher modes can also be useful to improve the accuracy on the velocity model at shallow depths, which is in most cases very low. Some of these issues have been raised by Ermert *et al.* (2014), but a full 2-D inversion strategy that would account for such information still has to be defined.

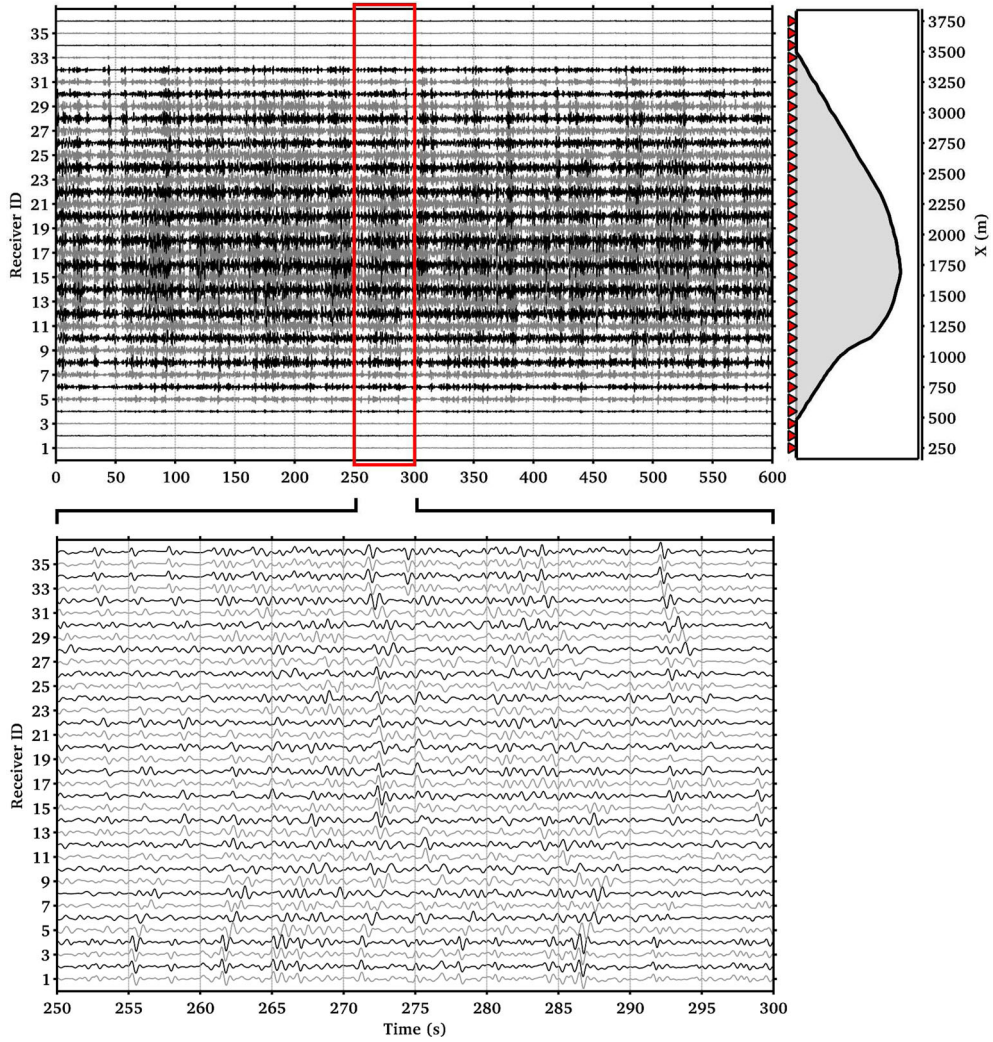


Figure 10. Stochastic simulation of ambient vibration recordings from the Martigny model. On top the whole simulation is plotted (36 traces, equal normalization), while on the bottom a 50 s zoom window (normalized to trace maximum) is shown.

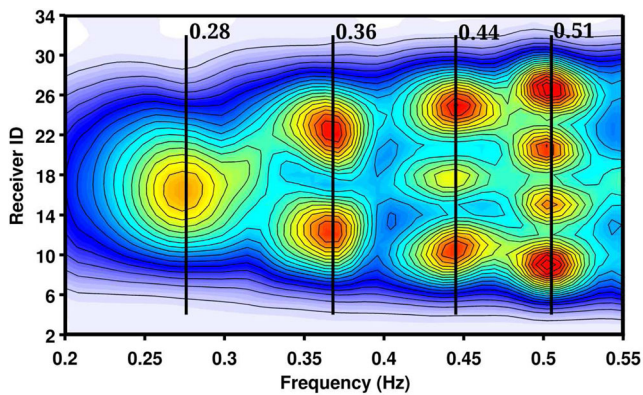


Figure 11. Standard spectral ratios of the synthetic ambient vibration recordings of Martigny. As reference we used the first receiver of the array, which sits on theoretical bedrock. Fundamental mode and first three overtones can easily be identified on the spectrum, together with the locations of the antinodal points along the profile.

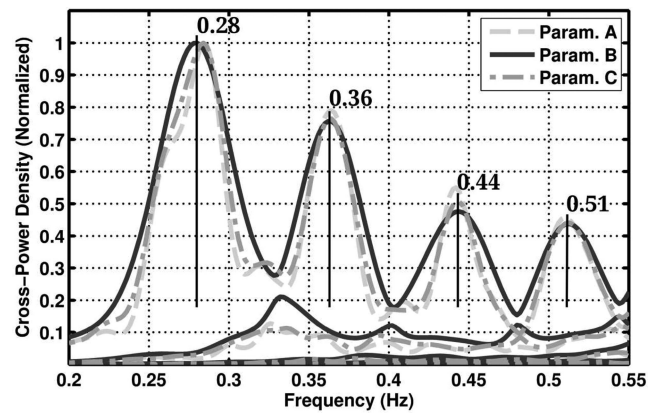


Figure 12. FDD eigenvalue spectrum of the simulated linear array of Martigny. Identified resonance frequencies are compatible with the results from SSR (Fig. 11). A sensitivity test was performed comparing different window length/number. Selected results are from parametrization B, with same window length as in the processing scheme used for real recordings (Table 2).

Table 2. Parameters for the sensitivity test performed comparing different window length/number.

Scheme	Window length (s)	Number of stacked windows
A	25	47
B	50	23
C	40	29

Table 3. Comparison of the first four resonance frequencies identified using FDD on observed (Obs) and simulated (Syn) recordings of the Martigny linear array.

	SH_{00} (Hz)	SH_{01} (Hz)	SH_{02} (Hz)	SH_{03} (Hz)
Obs.	0.29	0.38	0.44	0.51
Syn.	0.28	0.36	0.44	0.51

6 DISCUSSION AND CONCLUSIONS

In this paper, we discuss the effectiveness of an alternative approach to assess the resonance characteristics of 2-D basin structures through spectral decomposition of synchronous array recordings of ambient vibrations. As major outcome of the proposed method, it is now possible to obtain, together with the information about the resonance frequencies of the structure, the corresponding modal shapes. In particular, the location of nodes and antinodes of the resonant wavefield can now be correctly represented. This is hardly obtain-

able with simpler spectral techniques and using ambient vibrations, as for SSRs. Comparing results obtained from direct observation and from synthetic Green's function computation demonstrated the high resolving power and accuracy of FDD technique as a tool for site response analysis and ground motion prediction. Moreover, the method proved to be advantageous especially in urban environments and in low-seismicity regions, as the use of ambient vibration makes the survey of simple implementation (the acquisition time is only limited to few hours) and relatively inexpensive (no necessity of artificial source).

As evident from the processing, the spatial sampling of the wavefield at the surface plays a major role on the quality of the final result. Modal-shape discrimination is facilitated, as more sampling points per wavelength are considered. Consequently, low-energy higher-modes of the structure are potentially better resolved when using a denser spatial sampling. In this study, using 10 stations allowed retrieving modes up to 6th overtone very reliably, but additional modes can possibly be obtained by using additional receivers or closer station configurations (e.g. investigating smaller portion of the valley at a time). Complementary, the duration of the analysed signal has a direct influence on the statistical significance of the result. With a 2-hr measurement, sufficiently stable results have been obtained for the investigated frequency range. Using long recordings is generally advisable in presence of strong uncorrelated noise (e.g. in cities). In such a case, higher-modes can emerge from the spectrum only with longer window stacking, due to the improved signal-to-noise ratio. Here, nearly 2000 periods of the fundamental

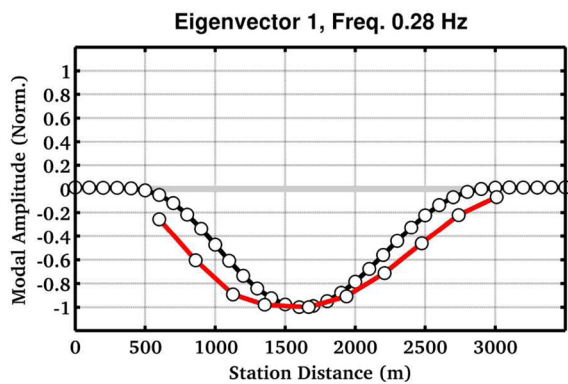
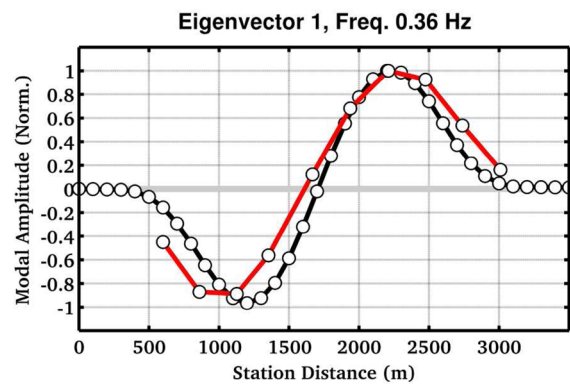
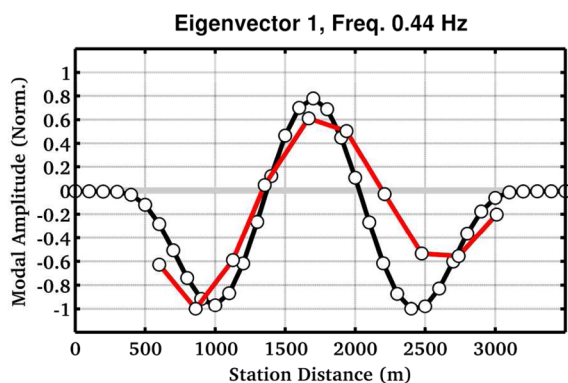
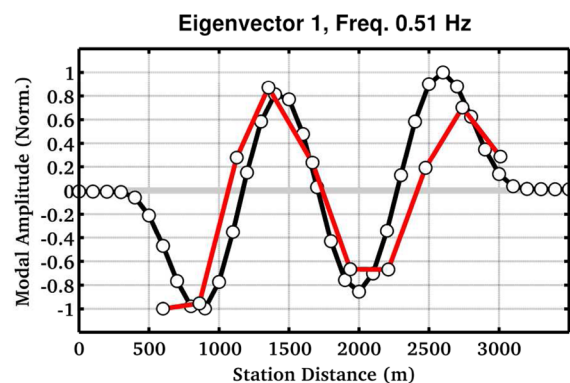
1) SH_{00} 1) SH_{01} 1) SH_{02} 1) SH_{03} 

Figure 13. Comparison between modal shapes from FDD analysis of real (in red) and simulated (in black) ambient vibration recordings of the Martigny site. White dots indicate the measuring location along the array (adjusted to match the different coordinate systems of the real and the simulated array). Frequency values from the synthetic case are shown as reference.

mode have been recorded, which corresponds to what is generally advised in the civil engineering literature (1000–2000, according to Cantieni 2005).

One open question is the possibility of identifying *SH* modes with nodes in the vertical direction (e.g. *SH*₁₀, according to the nomenclature of Bard & Bouchon (1985)). In this study no evidence of this phenomenon—which is theoretically predicted—is given. Several explanations can be proposed. The hypothesis that modes with nodes in the vertical direction have too similar frequencies with respect to their horizontal counterpart (and could therefore not be distinguished) is neglected by simple analytic examples provided by Bard & Bouchon (1985), as well as numerical modal analysis (Ermert *et al.* 2014). Most likely, the energy of such modes is relatively low, as they are not fully excited. This would explain why they do not emerge on the spectral decomposition, as their presence is masked by the development of dominant modes with nodes in horizontal direction. Moreover, Ermert *et al.* (2014) observed that nodes in vertical direction only occur quite ‘late’ in the modal sequence, that is at relatively high frequencies, for basins with strong velocity gradients in the uppermost part. This might be the case for Martigny. Alternatively, the formal separation of these two kinds of modes might be an unrealistic oversimplification in complex 2-D structures, for example in the case of strongly asymmetric valleys or with laterally heterogeneous infill.

As possible follow-up of this study, we plan to validate the reliability of the FDD method in the case of *P–SV* motion. Ermert *et al.* (2014) performed a test on real recordings, but an accurate comparison with results from a full numerical wave-propagation simulation is still missing. This will further improve our understanding and interpretation, as in such a case the partition of energy between the *P* and *SV* components leads to more complex modal patterns than the simple *SH* case. Further simulations will also be useful to further understand the sensitivity of 2-D modal shapes and resonance frequencies to the structural parameters of the model, in order to access the possibility of using such information for direct inversion of the soil properties. The next step will be then extending the analysis to the full three-component ground motion in complex 3-D media. Additionally, given the demonstrated high resolution of the method, FDD modal analysis might also be useful to directly predict surface ground motion, for instance by empirically retrieve the approximated linear response of the system using the modal superposition principle and complementary to quantify the presence of non-linearity, as reported in Guéguen *et al.* (2011).

ACKNOWLEDGEMENTS

We would like to acknowledge the contribution of Daniel Roten who has made the array data available to us. We extend our thanks to reviewers Dino Bindi and Philippe Guéguen and to Associate Editor Andrea Morelli, whose comments helped significantly improve this paper. This work was partly funded by the Swiss Federal Nuclear Safety Inspectorate (ENSI). Fig. 1 in this paper was made using Generic Mapping Tools (GMT) 4 software written by Wessel & Smith (1998).

REFERENCES

- Anderson, J.G., Bodin, P., Brune, J.N., Prince, J., Singh, S.K., Quaas, R. & Onate, M., 1986. Strong ground motion from the Michoacan, Mexico, earthquake, *Science*, **233**, 1043–1049.
- Anderson, J.G., Lee, Y., Zheng, Y. & Day, S., 1996. Control of strong motion by the upper 30 meters, *Bull. seism. Soc. Am.*, **86**, 1749–1759.
- Asten, M.W., 2006. Site shear velocity profile interpretation from microtremor array data by direct fitting of SPAC curves, in *Proceedings of the Third International Symposium on the Effects of Surface Geology on Seismic Motion (ESG2006)*, Grenoble, France, 30 August–1 September 2006, Vol. 1, Paper Number 99.
- Asten, M.-W. & Henstridge, J.-D., 1984. Array estimators and the use of microseisms for reconnaissance of sedimentary basins, *Geophysics*, **49**, 1828–1837.
- Bard, P.-Y. & Bouchon, M., 1985. The two-dimensional resonance of sediment-filled valleys, *Bull. seism. Soc. Am.*, **75**(2), 519–541.
- Bard, P.-Y. & Gariel, J.C., 1986. The seismic response of two-dimensional sedimentary deposits with large vertical velocity gradients, *Bull. seism. Soc. Am.*, **76**, 343–366.
- Bindi, D. *et al.*, 2009. Site amplifications observed in the Gubbio Basin, Central Italy: hints for lateral propagation effects, *Bull. seism. Soc. Am.*, **99**(2A), 741–760.
- Bohlen, T., 2002. Parallel 3-D viscoelastic finite-difference seismic modelling, *Comput. Geosci.*, **28**(8), 887–899.
- Bonnefoy-Claudet, S., Cotton, F. & Bard, P.-Y., 2006. The nature of noise wavefield and its applications for site effects studies: a literature review, *Earth-Sci. Rev.*, **79**, 205–227.
- Borcherdt, R.D., 1970. Effects of local geology on ground motion near San Francisco Bay, *Bull. seism. Soc. Am.*, **60**, 29–61.
- Brincker, R., Zhang, L. & Andersen, P., 2001. Modal identification of output-only systems using frequency domain decomposition, *Smart Mater. Struct.*, **10**(3), 441–445.
- Burjnek, J., Gassner-Stamm, G., Poggi, V., Moore, J.R. & Fäh, D., 2010. Ambient vibration analysis of an unstable mountain slope, *Geophys. J. Int.*, **180**(2), 820–828.
- Cantieni, R., 2005. Experimental methods used in system identification of civil engineering structures, in *Proceedings of the 1st IOMAC, International Operational Modal Analysis Conference*, April 26–27, Copenhagen, Denmark, pp. 249–260.
- Chavez-Garcia, F.J., Raptakis, D., Makra, K. & Pitilakis, K., 2000. Site effects at Euroseistest-II. Results from 2D numerical modelling and comparison with observations, *Soil Dyn. Earthq. Eng.*, **19**(1), 23–39.
- Cornou, C., 2004. Simulation for real sites: set of noise synthetics for H/V and array studies from simulation of real sites and comparison for test sites, SESAME Deliverables D11.10 & D17.10, SESAME EVG1-CT-2000–00026 project, 62 pp.
- Ermert, L., Poggi, V., Burjánek, J. & Fäh, D., 2014. Fundamental and higher 2-D resonance modes of an Alpine valley, *Geophys. J. Int.*, **198**(2), 795–811.
- Fäh, D. & Suhadolc, P., 1994. Application of numerical wave-propagation techniques to study local soil effects: the case of Benevento (Italy), *Pure appl. Geophys.*, **143**(4), 513–536.
- Field, E.H., 1996. Spectral amplification in a sediment-filled valley exhibiting clear Besin-edge induced waves, *Bull. seism. Soc. Am.*, **86**, 991–1005.
- Frischknecht, C. & Wagner, J.-J., 2004. Seismic soil effect in an embanked deep Alpine Valley: a numerical investigation of two-dimensional resonance, *Bull. seism. Soc. Am.*, **94**(1), 171–186.
- Géli, L., Bard, P.-Y. & Jullien, B., 1988. The effect of topography on earthquake ground motion: a review and new results, *Bull. seism. Soc. Am.*, **78**(1), 42–63.
- Goulet, J.-A., Michel, C. & Smith, I.F.C., 2013. Hybrid probabilities and error-domain structural identification using ambient vibration monitoring, *Mech. Syst. Signal Pr.*, **37**(1–2), 199–212.
- Guéguen, P., Cornou, C., Garambois, S. & Banton, J., 2007. On the limitation of the H/V spectral ratio using seismic noise as an exploration tool: application to the Grenoble Valley (France), a small apex ratio basin, *Pure appl. Geophys.*, **164**(1), 115–134.
- Guéguen, P., Langlais, M., Foray, P., Rousseau, C. & Maury, J., 2011. A natural seismic isolating system: the buried mangrove effects, *Bull. seism. Soc. Am.*, **101**(3), 1073–1080.
- Hisada, Y. & Yamamoto, S., 1996. One-, two- & three-dimensional site effects in sediment-filled basins, in *Proceedings of the 11th World Conference on Earthquake Engineering*, Acapulco, Mexico.

- Ibs-von Seht, M. & Wohlenberg, J., 1999. Microtremor measurements used to map thickness of soft sediments, *Bull. seism. Soc. Am.*, **89**, 250–259.
- Joyner, W.B., Warrick, R.E. & Fumal, T.E., 1981. The effect of Quaternary alluvium on strong ground motion in the Coyote Lake, California earthquake of 1979, *Bull. seism. Soc. Am.*, **71**, 1333–1349.
- Kagami, H., Duke, C.M., Liang, G.C. & Ohta, Y., 1982. Observation of 1 to 5 second microtremors and their application to earthquake engineering. Part 2. Evaluation of site effect upon seismic wave amplification due to extremely deep soil deposits, *Bull. seism. Soc. Am.*, **72**, 987–998.
- King, J. & Tucker, B., 1984. Observed variations of earthquake motion over a sediment-filled valley, *Bull. seism. Soc. Am.*, **74**, 173–152.
- Lachet, C. & Bard, P.-Y., 1994. Numerical and theoretical investigations on the possibilities and limitations of Nakamura's technique, *J. Phys. Earth*, **42**, 377–397.
- Lermo, J. & Chavez-Garcia, F.J., 1994. Are microtremors useful in site response evaluation?, *Bull. seism. Soc. Am.*, **84**, 1350–1364.
- Le Roux, O., Jongmans, D., Cornou, C. & Schwartz, S., 2012. 1D and 2D resonances in an Alpine valley identified from ambient noise measurements and 3D modelling, *Geophys. J. Int.*, **191**, 579–590.
- Michel, C., Guéguen, P., El Arem, S., Mazars, J. & Kotronis, P., 2010. Full-scale dynamic response of an RC building under weak seismic motions using earthquake recordings, ambient vibrations and modelling, *Earthq. Eng. Struct. Dyn.*, **39**(4), 419–441.
- Pfiffner, O.A., Heitzmann, P. & Frei, W., 1997. *Deep Structure of the Swiss Alps: Results of NRP 20*, Birkhäuser.
- Poggi, V. & Fäh, D., 2010. Estimating Rayleigh wave particle motion from three-component array analysis of ambient vibrations, *Geophys. J. Int.*, **180**, 251–267.
- Poggi, V., Fäh, D., Burjanek, J. & Giardini, D., 2012. The use of Rayleigh wave ellipticity for site-specific hazard assessment and microzonation. An application to the city of Luzern (Switzerland), *Geophys. J. Int.*, **188**(3), 1154–1172.
- Roten, D. & Fäh, D., 2007. A combined inversion of Rayleigh wave dispersion and 2-D resonance frequencies, *Geophys. J. Int.*, **168**(3), 1261–1275.
- Roten, D., Fäh, D., Cornou, C. & Giardini, D., 2006. Two-dimensional resonances in Alpine valleys identified from ambient vibration wavefields, *Geophys. J. Int.*, **165**(3), 889–905.
- Smerzini, C., Paolucci, R. & Stupazzini, M., 2011. Comparison of 3D, 2D and 1D numerical approaches to predict long period earthquake ground motion in the Gubbio plain, Central Italy, *Bull. Earthq. Eng.*, **9**(6), 2007–2029.
- Steimen, S., Fäh, D., Kind, F., Schmid, C. & Giardini, D., 2003. Identifying 2D resonance in microtremor wave field, *Bull. seism. Soc. Am.*, **93**(2), 583–599.
- Trifunac, M.D. & Brady, A.G., 1975. A study on the duration of strong earthquake ground motion, *Bull. seism. Soc. Am.*, **65**, 581–626.
- Vidale, J.E., 1986. Complex polarization analysis of particle motion, *Bull. seism. Soc. Am.*, **76**, 1393–1405.
- Vidale, J.E. & Helmberger, D.V., 1988. Elastic finite-difference modeling of the 1971 San Fernando, California, earthquake, *Bull. seism. Soc. Am.*, **78**, 122–141.
- Wessel, P. & Smith, W.H.F., 1998. New, improved version of the generic mapping tools released, *EOS, Trans. Am. geophys. Un.*, **79**, 579.
- Yamanaka, H., 1993. Continuous measurement of microtremors on sediments and basement in Los Angeles, *Bull. seism. Soc. Am.*, **83**, 1595–1604.